Journal of CO2 Utilization 67 (2023) 102347

Contents lists available at ScienceDirect

Journal of CO2 Utilization

journal homepage: www.elsevier.com/locate/jcou

Atomic oxygen assisted CO_2 conversion: A theoretical analysis

C. Verheyen [a,b,*], K. van 't Veer [a], R. Snyders [b,c], A. Bogaerts [a]

[a] PLASMANT, Department of Chemistry, University of Antwerp, Belgium
[b] Plasma-Surface Interaction Chemistry, University of Mons, 23 Place du Parc, 7000 Mons, Belgium
[c] Materia Nova Research Center, 3 Avenue Nicolas Copernic, 7000 Mons, Belgium

ARTICLE INFO

Keywords:
CO2
Oxygen
Climate change
SDG
Conversion

ABSTRACT

With climate change still a pressing issue, there is a great need for carbon capture, utilisation and storage (CCUS) methods. We propose a novel concept where CO_2 conversion is accomplished by O_2 splitting followed by the addition of O atoms to CO_2. The latter is studied here by means of kinetic modelling. In the first instance, we study various CO_2/O ratios, and we observe an optimal CO_2 conversion of around 30–40% for 50% O addition. Gas temperature also has a large influence, with a minimum temperature of around 1000 K to a maximum of 2000 K for optimal conversion. In the second instance, we study various CO_2/O/O_2 ratios, due to O_2 being a starting gas. Also here we define optimal regions for CO_2 conversion, which reach maximum conversion for a CO_2 fraction of 50% and an O/O_2 ratio bigger than 1. Those can be expanded by heating on one hand, for low atomic oxygen availability, and by quenching after reaction on the other hand, for cases where the temperatures are too high. Our model predictions can serve as a guideline for experimental research in this domain.

1. Introduction

In May 2021 the National Oceanic and Atmospheric Administration (NOAA) measured the highest recorded CO_2 concentrations at 419 ppm up to then. [1] This is almost a 50% increase from pre-industrial levels, which are estimated at 280 ppm. [2] This brings us closer to the crucial limit of a 1.5 °C increase in global temperature. [3] Passing this point would lead to unprecedented weather events, sea levels rising due to melted ice-caps, deaths of many species, many climate refugees and increased inequality, to sum up, a few examples. [3] The call for climate action is very urgent and has also been put forward as one of the sustainable development goals (SDG) [4] by the United Nations (SDG 13). Moreover, it is intertwined with many other SDGs, for example, life below water (SGD 14) and clean energy (SDG 7). [5] To stay below the 1.5 °C limit, high concentrations of CO_2 need to be tackled. This is due to the "greenhouse heating effect' of the molecule, combined with its longevity and stability. [6].

A combined strategy of carbon mitigation, adaptation and carbon capture and utilization and storage (CCUS) is preferred to stop the levels from increasing [3], together with an effort in bringing the existing CO_2 levels down – through negative emissions technology (NET). [7] To bring this into implementation, there is a need for good policies together with the development of new CCUS methods and improvement of existing ones. [3] If possible, carbon capture should take place already at (pre-)exhaust level (pre-, post-and oxy-combustion), thus it allows for capturing the emissions at the moment they are released. [8] Carbon capture and storage (CCS) allows for the removal of CO_2 from the atmosphere but misses a big opportunity for the re-utilization of the carbon. [9] Carbon capture and utilisation (CCU) is an interesting way of combatting climate change, as it allows for the re-utilization of already emitted CO_2 and it could be an alternative carbon source to fossil fuels. [10] This fits perfectly into a framework for a circular economy and is thus a very interesting path forward for the future. [11].

Many methods for CCU have been developed over the years: electrochemical, solar thermochemical, biochemical and photochemical conversion, as well as hybrid methods. [10,12] Each approach has its benefits, but all of them struggle with difficulties related to e.g., catalyst instabilities, the use of rare materials, cultivation problems,… In short, the presented methods are capable of converting CO_2 but sometimes require complex set-ups and thus high investment costs and often have limited scale-up possibilities. [12].

On the other hand, gas conversion offers a relatively simple way of converting CO_2. It uses CO_2 in gaseous form without the addition of non-gaseous products (like binding metals) that are needed for conversion. Examples are thermal and plasma conversion. Thermal conversion allows for high conversion rates, but at low energy efficiency. [12] This is

* Corresponding author at: PLASMANT, Department of Chemistry, University of Antwerp, Belgium.
E-mail address: claudia.verheyen@uantwerpen.be (C. Verheyen).

https://doi.org/10.1016/j.jcou.2022.102347
Received 26 July 2022; Received in revised form 14 November 2022; Accepted 28 November 2022
2212-9820/© 2022 The Authors. Published by Elsevier Ltd. This is an open access article under the CC BY-NC-ND license (http://creativecommons.org/licenses/by-nc-nd/4.0/).

due to the stability of the CO_2 molecule and thus a great amount of energy is needed to break the double bonds (R1). [13].

$$CO_2 \rightarrow CO + O \ \Delta H^\circ = 5.5\ eV/molecule \quad (R1)$$

The O atom formed in R1 can also react with CO_2, leading to the dissociation of the latter:

$$CO_2 + O \rightarrow CO + O_2 \ \Delta H^\circ = 0.3\ eV/molecule \quad (R2)$$

The sum of both reactions gives us:

$$CO_2 \rightarrow 2\ CO + O_2 \ \Delta H^\circ = 5.8\ eV/molecule \quad (R3)$$

Or in reduced form.

$$CO_2 \rightarrow CO + ½\ O_2 \ \Delta H^\circ = 2.9\ eV/molecule \quad (R4)$$

The indirect route (R2) offers some insight into possible optimisations of the conversion, because of the much lower reaction enthalpy.

Besides thermal conversion, another way to optimise gas conversion is the use of plasma technology. [12] Plasma will allow for conversion through different channels, like electron-impact dissociation or the more efficient vibrational ladder-climbing. [14] This allows for the addition of energy to the vibrational levels. Subsequently, through collisions, vibrational energy will be exchanged between molecules, allowing some molecules to become more excited until they reach the highest vibrational level, which then leads to dissociation. [15] Different types of plasma reactors, like microwave (MW), gliding arc (GA), dielectric barrier discharge (DBD), etc. can be used. Plasma conversion allows for reaching quite high energy efficiencies, depending on the plasma type. Indeed, up to 90% was reported in MW plasmas. [16] However, this was at specific conditions (reduced pressure and supersonic flow) and has not been reproduced since then. Moreover, high energy efficiency is not always associated with high conversion, and more research is needed to improve the performance of plasma-based CO_2 conversion. [12] In general, every CCU method mentioned is characterised by successes, but also needs further improvement.

All those methods have in common that the focus is on the CO_2 molecule as the main energy-consuming compound. Alternatively, instead of focusing on how to split the CO_2 molecule by applying energy to it, a deeper look into the most favourable reactions for CO_2 splitting could possibly allow for a simpler solution for CO_2 conversion.

As mentioned above, the indirect route (reaction R2) has a much lower reaction enthalpy. Therefore, increasing the occurrence of this reaction could lead to better conversion and energy efficiency. Indeed, previous studies [17,18] have found that atomic oxygen plays a positive role in plasma-based CO_2 conversion, due to so-called super-ideal quenching. This concept was brought forward in the plasma chemistry community by Fridman. [13].

Therefore, we propose here to start with atomic oxygen as the biggest driving force for CO_2 conversion. Step 1 would consist of converting O_2 into O, by utilizing e.g., plasma, heat, UV or any other suitable method. This is in theory less energy-consuming than CO_2 splitting (the O=O dissociation bond energy is 498 kJ/mol vs 532.2 kJ/mol for the OC=O bond dissociation energy at 298 K) [19]. Step 2 would be the addition of CO_2 into this stream of O atoms, or the O_2/O mixture, allowing the reaction (R2) to be dominant. By adding O atoms to pure CO_2 gas, instead of a CO_2/CO mixture (i.e., already partially converted CO_2), the backward reaction of (R1) can be, in the first instance, bypassed. The difference with previous works, as mentioned above, is that the focus here is to provide the O-atoms externally (thus a source separate from the CO_2) to optimize reaction R2.

Our hypothesis is that this process of creating O atoms, to let them react with CO_2 gas, could be a promising and more energy-efficient novel route for CO_2 conversion. To test this hypothesis, we explore here theoretically the second step of this process, i.e., reaction (R2), by means of modelling, in an attempt to define this novel concept and lay down a basis for further research.

2. Methods

The chemical reactions are described by a 0D chemical kinetics model in the Fortran 90 ZDPlasKin (Zero-Dimensional Plasma Kinetics solver) code. [20] The model calculates density changes for all different species in the model, in a homogeneous volume element over time. It includes gas heating but neglects physical parameters related to transport. Therefore, only the mass conservation equation for every species and the gas thermal balance equation are solved. The density changes over time can be represented by:

$$\frac{dn_s}{dt} = \sum_{j=1}^{j_{max}} Q_{sj} = \sum_{j=1}^{j_{max}} R_j \left[a_{sj}^R - a_{sj}^L\right], \quad (1)$$

$$R_j = k_j \prod_l n_l, \quad (2)$$

where n_s is the density of the species s, Q_{sj} is the source term for reaction j of the species s, a_{sj}^R and a_{sj}^L represent the stoichiometric coefficients on the right and left sides, respectively, of species s for reaction j. R_j is the reaction rate and k_j the reaction rate coefficient.

The gas heating can be calculated as:

$$N \frac{\gamma k_B}{\gamma - 1} \frac{dT_{gas}}{dt} = \sum_{j=1}^{j_{max}} \Delta H_j * R_j - P_{ext}, \quad (3)$$

where N is the total gas density, γ is the specific gas heat ratio, k_B is the Boltzmann constant, ΔH_j is the enthalpy released or consumed during reaction j, and P_{ext} is the external cooling.

The rate coefficients of the reactions between molecules, atoms and excited species are temperature-dependent and obtained from the literature (see below).

There is no addition of power, thus the changes are chemically driven. However, one could argue that the addition of atomic oxygen is an indirect way of adding power. Indeed, power is needed to first split O_2 into O atoms. As a result, we can calculate the energy efficiency (see derivation in the Appendix) of the process through

$$\eta = \frac{x_{CO_2}}{1 - x_{CO_2}} \frac{\chi_{CO_2}}{\chi_{O_2}} \frac{\Delta H_{CO_2}}{\Delta H_{O_2}} \quad (4)$$

where η represents the energy efficiency, x represents the fraction in the gas, χ the conversion and ΔH the dissociation energy.

The calculations are performed over time, for a gas in a volume element, comparable to a batch reactor. However, by means of a gas velocity, the time dependence in a batch reactor can also be translated to spatial dependence, i.e., as a function of distance travelled through a (tubular) reactor, because of the equivalence between batch reactor and plug flow reactor in terms of residence time and distance travelled through the reactor. Hence, the calculations can mimic the situation of continuous flow reactors where O atoms (or an O/O_2 mixture) and CO_2 gas are brought in contact.

The chemistry described in the model includes the species listed in Table 1. They react with each other in 19 base reactions, which are listed in the Appendix. The chemistry is based on previous work from our group. [21] This allows for usage in multiple conditions and an easier transition for future research. Besides neutral ground-state species, it also includes various vibrationally excited levels of the molecules, which

Table 1
Most important species included in the model for the CO_2 gas reacting with O atoms or an O/O_2 mixture.

Neutral ground state species
O_2, O, CO_2, CO, C
Excited species
$O_2[V_1\text{-}V_4]$, $CO[V_1\text{-}V_{10}]$, $CO_2[V_1\text{-}V_{21}]$, $CO_2[V_a\text{-}V_d]$

can be easily populated at the higher temperatures under study in this work. Note that electronically excited levels of O are not included, as they would be negligible at the conditions under study. The notations of these levels are explained in our earlier work. [21].

The model is on purpose kept simple to give more insight into the basic chemical reactions and changes that occur by the mixing of O atoms (or an O/O_2 mixture) with CO_2 gas at room temperature and to lay the groundwork for experimental studies. Note in fact that the vibrationally excited molecules of O_2, CO and CO_2 could also be simply described by a Boltzmann distribution, as our model is applied to a gas, and not to a plasma, so the vibrational distribution functions of these molecules are determined by the gas temperature. In the results section (Section 3 c), we provide a sensitivity analysis, where we compare the results without vibrational levels, showing that they yield the same results.

3. Results and discussion

3.1. CO_2 conversion upon reaction with O atoms

To explore CO_2 conversion driven by O atoms, and thus to prove the aforementioned concept, we consider a simple approach of mixing CO_2 and O and we follow the changes of the mixture over time. It should be noted that no external power is applied in these calculations, as would be the case when e.g., a plasma is created; hence, only chemical reactions take place. The results can be found in Fig. 1. Fig. 1A illustrates the CO_2 conversion in different CO_2/O mixtures, for different concentrations of O atoms upon mixing (t = 0 s). For instance, the addition of 30% O atoms yields a CO_2 conversion of 10%, simply by chemical reactions (reaction (R2) in the Introduction). The higher the O fraction, the higher the CO_2 conversion is reached in short timescales. Indeed, a CO_2 conversion up to almost 100% can be achieved upon the addition of 90% O atoms, simply by thermal chemistry, without the addition of external power. However, this conversion drops as a function of time (as explained below), and is thus not practical in an industrial setup. The highest conversion, when looking at a longer timescale and steady-state, is achieved at a ratio of 50/50 CO_2/O, reaching a value of up to 40%.

Fig. 1B depicts the gas temperature, self-consistently calculated for the different CO_2/O mixtures, and provides good insight into the underlying mechanisms, especially in the case of high conversions (60% and higher). Upon mixing CO_2 with O, the gas is at room temperature, but before the O atoms will be able to react with CO_2 molecules (reaction (R2) from the Introduction, which is an endothermic reaction), a fraction of them will recombine with other O atoms (R5):

$$O + O \rightarrow O_2 \quad \Delta H^\circ = -5.2\ eV/molecule \tag{R5}$$

The recombination of O atoms (R5) is an exothermic reaction, which easily proceeds at room temperature, and leads to a temperature rise, as clearly observed in Fig. 1B. As a result, the endothermic reaction

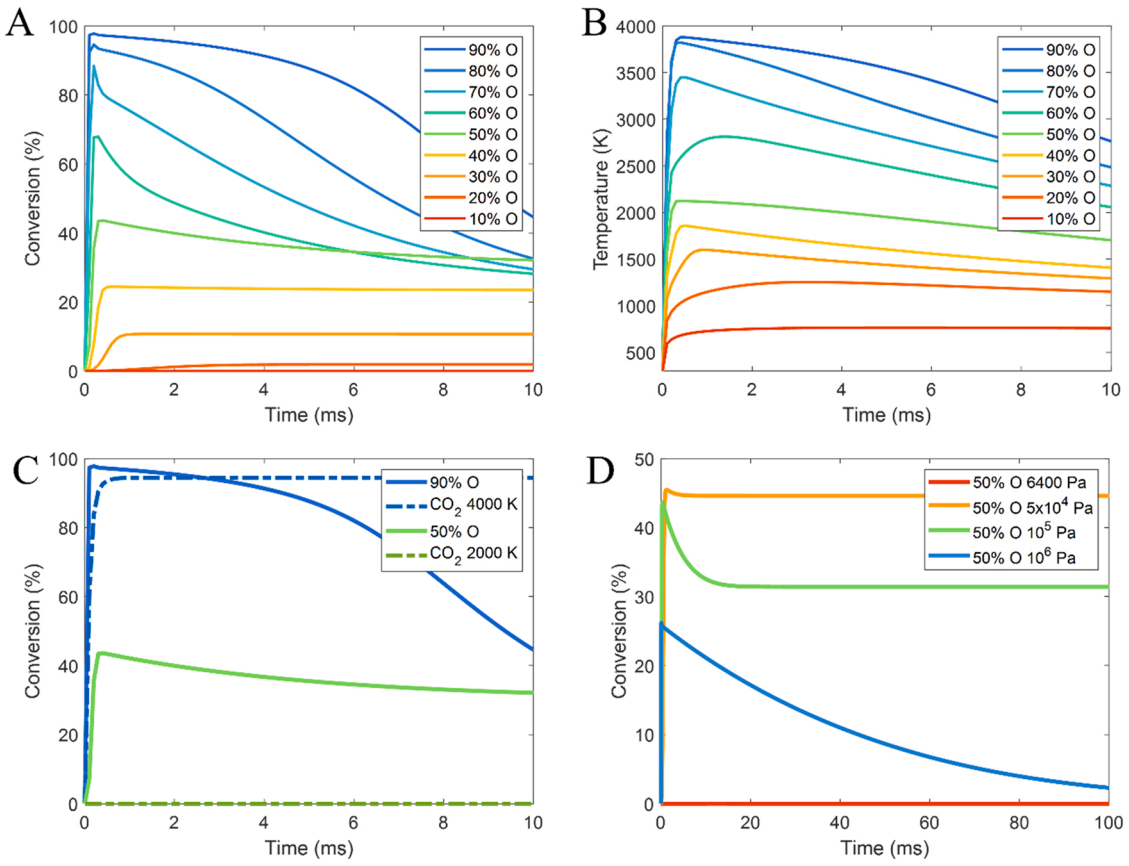


Fig. 1. Overview of CO_2 conversion upon addition of O atoms: A) Conversion of CO_2 in a CO_2/O mixture: addition of O in higher concentrations results in higher conversion at first. However, the conversion drops after a few ms for the higher O fractions (above 50%), while up to 50% O fraction, it stays rather constant. B) Gas temperature self-consistently calculated for the CO_2/O mixtures of (A): The addition of more O atoms results in higher gas temperatures, due to the heat created by O-O recombination into O_2 (see text). Full figures of (A) and (B) can be found in the Appendix. C) Comparison of pure CO_2 conversion at fixed temperatures of 2000 and 4000 K (dashed lines) with CO_2/O conversion for 50% and 90% O fraction (solid lines), which yield self-consistent temperatures around 2000 and 4000 K, respectively (cf. B): when we remain below the thermal conversion limit for CO_2, e.g., in case of the 50/50 CO_2/O mixture (2000 K), we see a dramatic increase from roughly 0% conversion up to 40% conversion. Above the thermal conversion limit (e.g., in case of 90% O, 4000 K), we see no improvement. D) CO_2/O conversion at different pressures for 50% O fraction: an intermediate pressure around 5×10^4 Pa is optimal, indicating the importance of collision frequency and gas temperature (see text).

between CO_2 and O (R2) can take place, resulting in CO_2 conversion (see Fig. 1A). For high O fractions, however, the temperature can rise above 3000 K, which reflects the CO_2 thermal conversion limit (i.e., reaction step (R1)). In this case, the temperature rise serves therefore a double purpose. On one hand, it is clear that the conversion upon addition of O atoms is partly due to the increase in temperature, giving rise to purely thermal conversion (at a high enough O fraction), but on the other hand, and more importantly, even at lower O fractions, when the temperature is below the thermal conversion limit of around 3000 K, it already provides enough energy for reaction (R2, the reaction of CO_2 with O atoms) to proceed, which is only slightly endothermic, and thus requires less energy.

To confirm that the conversion is not purely thermal, but proceeds by reaction (R2), at least for temperatures below the thermal conversion limit, we compare in Fig. 1C our CO_2/O calculations with pure CO_2 chemical kinetics simulations at similar temperatures. Indeed, we compare two cases, i.e., 50% and 90% O fraction: at 50% O fraction, the self-consistently calculated gas temperature rises to about 2000 K due to the exothermic O atom recombination reaction, while at 90% O fraction, the gas temperature rises to almost 4000 K (see Fig. 1B). Hence, we compare in Fig. 1C the conversion in the CO_2/O mixtures at 50% and 90% O fraction with the corresponding thermal conversion in pure CO_2 at 2000 K and 4000 K, respectively. At 50% O fraction, we obtained 40% CO_2 conversion (see also Fig. 1A), while the conversion in pure CO_2 at 2000 K is lower than 1%. This demonstrates that the conversion in the CO_2/O mixture is not purely thermal (reaction (R1)), but is mainly due to the reaction of CO_2 with O atoms (R2), which is clearly less endothermic. However, for cases that are above the thermal conversion limit, i.e., at 90% O addition (reaching almost 4000 K), a similar conversion of 99% can be observed, indeed attributed to thermal conversion, though without an external heating source, but simply upon addition of O atoms. On the other hand, as the high temperature is not maintained over time and due to the presence of O/O_2, the conversion drops again due to backward reactions. Therefore, for CO_2/O conversion, too high temperatures (higher than 2500 K) seem to be counterproductive after the initial reaction phase.

Finally, the pressure and thus collision frequency is important for this concept. As mentioned before, reaction (R2) needs enough energy to proceed, and this can only be achieved when the exothermic O atom recombination reaction occurs to the right extent, i.e., sufficient to

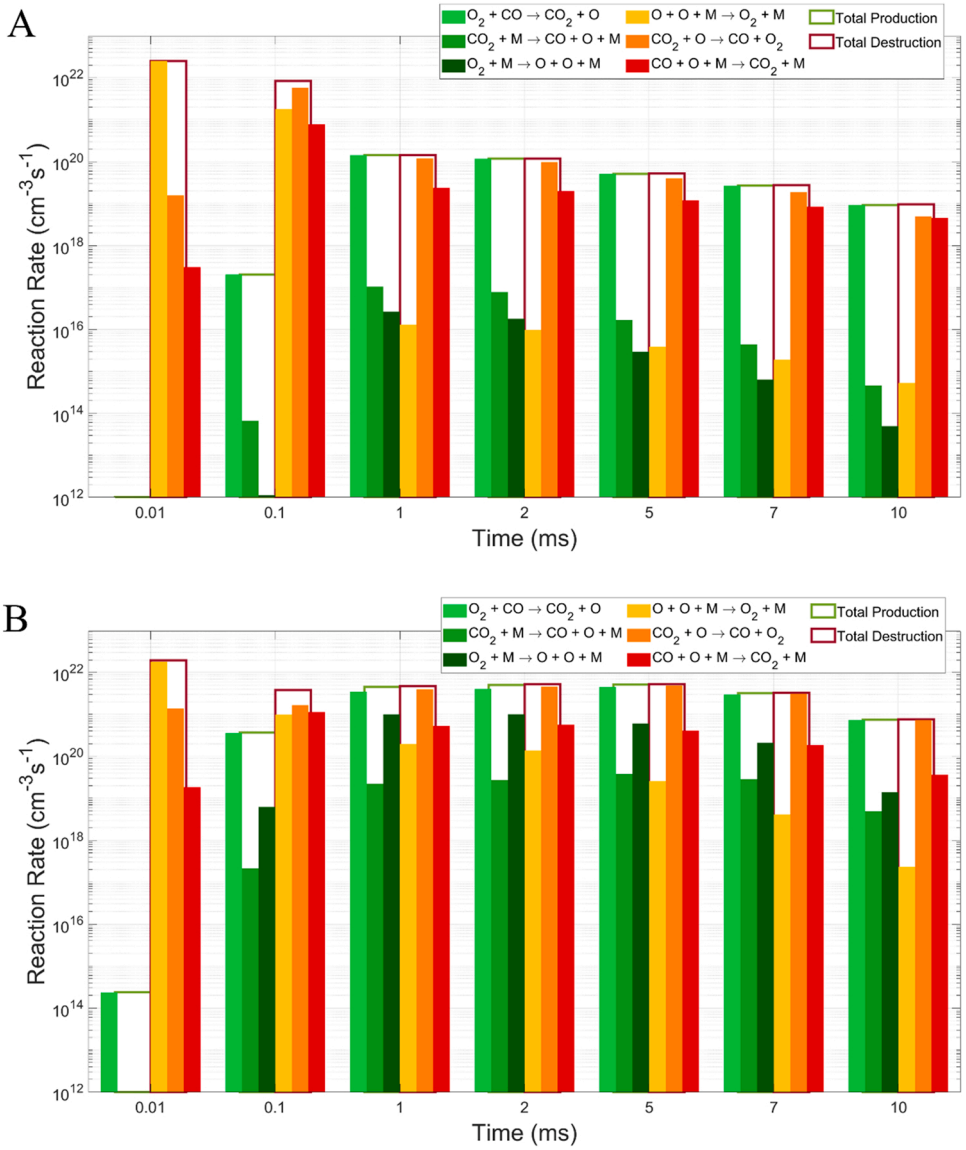


Fig. 2. Reaction rates of the most important production and destruction reactions for O atoms, as well as the total production and destruction rates. A) 50%, and B) 90% O atom addition.

provide enough heat, but without going over the thermal limit of CO_2, which would not lead to further gains after steady state. Thus, the interplay between pressure, CO_2/O mixing ratio and temperature is of great importance. Starting from room temperature, our calculations reveal that a pressure of 5×10^4 Pa is ideal for maximum conversion (see Fig. 1D). Indeed, lower pressures give rise to less O recombination, not providing enough heat for reaction (R2) to take place, while too high pressures give rise to too much O recombination, and hence too high temperatures that are not optimal for the process to occur (see above).

To obtain a deeper insight into the underlying reactions, we performed a reaction analysis of the destruction and production of O atoms, as presented in Fig. 2. Fig. 2A shows the most prevalent reactions for 50% O addition. We can observe that initially (t = 0.01 ms) the recombination of O atoms into O_2 is the most important destruction reaction, but already after 0.1 ms, reaction (R2), i.e., the conversion of CO_2 to CO, becomes more important. Finally, at longer timescales (t = 10 ms), this reaction is balanced by the recombination of O + CO, forming again CO_2. Hence, this reaction is limiting the CO_2 conversion. In addition, the most important O production reaction is the recombination of O_2 with CO, also forming again CO_2 as well as O. Note that this is the backward reaction of (R2). It is not important at early timescales, but from t = 1 ms, it becomes equal to (or even slightly higher than) the forward reaction of (R2). We can see that after 1 ms, the net production of O becomes almost 0, and with O being the driving force of this concept, this indicates the beginning of the formation of a steady-state and the halt in the increase of CO_2 conversion. Indeed, this is the point where CO_2 production will overtake the CO_2 conversion, the latter reaching a maximum at around 0.1 ms.

In the case of 90% O addition (Fig. 2B), the dynamic of O destruction and formation is slightly different. We still see that initially (t = 0.01 ms) the recombination of O atoms into O_2 is the most important, and that reaction (R2) quickly becomes equally important and takes over from t = 1 ms, and also will be balanced by its backward reaction from t = 1 ms, just like in the case of 50% O addition. However, because at 90% O addition, the O fraction highly outweighs the CO_2 fraction, this leads in the longer term as well to more O_2 in the mixture. Combined with the higher temperatures at 90% O addition (see Fig. 1B), this leads after a while to more O production than for the 50% O addition case, due to the dissociation of O_2 and reaction (R1) (see Fig. 2B: dark green and middle green bars, respectively).

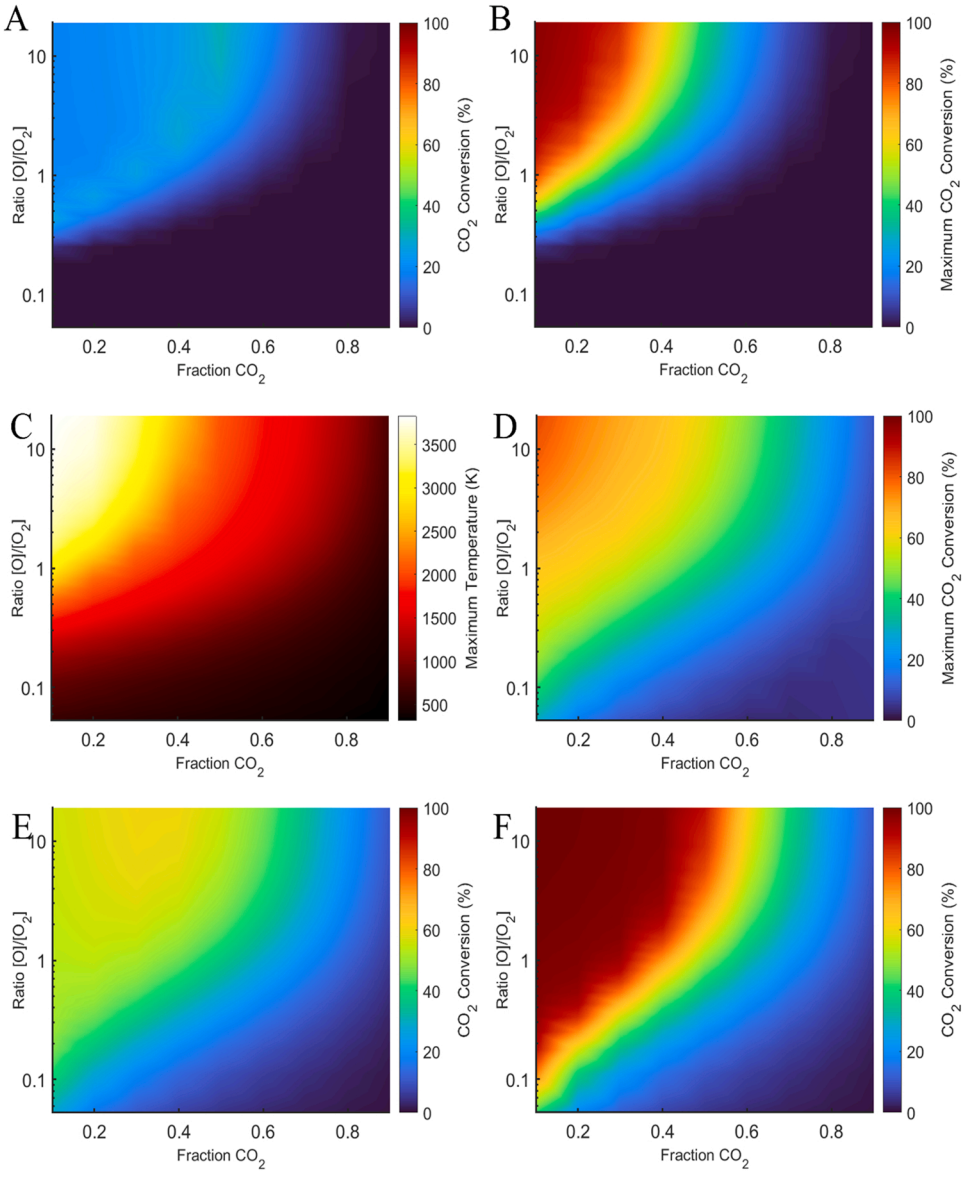


Fig. 3. Overview of CO_2 conversion as a function of the fraction of CO_2 in the mixture and the O/O_2 ratio, with (A-C) self-consistent calculation of temperature, and (D-E) fixed temperature of 2000 K. A) Conversion at steady state (1 s): The highest conversion (around 30%) is achieved at a 50% CO_2 fraction with an O/O_2 ratio above 6. B) Maximum conversion: The highest conversion (about 99%) is achieved at the lowest CO_2 fraction and high O/O_2 ratio. The high concentration of O atoms leads to high temperatures (over 3000 K) which lead to better (thermal) conversion at an early stage of mixing. C) Maximum temperature achieved in the model: lower CO_2 fractions and higher O/O_2 ratios lead to higher temperatures. D) Maximum conversion at constant temperature of 2000 K, highlighting the importance of a high enough temperature. Indeed, at 2000 K, higher CO_2 fractions and lower O/O_2 ratios allow already for good conversion, as compared to figure B, where the temperature is lower at these conditions (see figure C), and on the other hand, the conversion in Fig. D is lower than in Fig. B at lower CO_2 fractions and higher O/O_2 ratios, where the temperature is higher than 2000 K (see figure C). E) Conversion at steady state at 2000 K, with cooling to 300 K right after reaching the maximum. Cooling the setup allows for (partly) quenching the backward reactions, explaining the higher steady state conversion than in figure A. F) Conversion at 400 Pa after 1 s with constant temperature at 2000 K. Low pressure with higher temperature allows for high conversion.

3.2. CO_2 conversion upon mixing with an O_2/O mixture

Our model predictions of the previous section reveal that adding O atoms to CO_2 gas at room temperature can give rise to significant CO_2 conversions, e.g., around 40% for a 50/50 CO_2/O mixture, without adding external power or heating. However, mixing only O atoms with CO_2 gas, and thus achieving a 100% O_2 dissociation degree experimentally, can be hard to achieve. Therefore, to simulate the output of different methods for O atom production, we studied the effect of different [O]/[O_2] ratios, along with the CO_2 fraction in the mixture, on the CO_2 conversion, as illustrated in Fig. 3. The corresponding overall energy efficiency for the case of Fig. 3(A,B), as calculated by Eq. (4) above, is plotted in Appendix (Fig. A2). It reaches about 50%.

In Fig. 3A we show the conversions at steady-state, while Fig. 3B shows the maximum conversion that can be obtained. It is important to notice that (referring to Fig. 1A) the maximum is obtained quite early and is significantly higher than the steady-state values. However, the highest conversions drop quickly due to backward (recombination) reactions, so they would be harder to achieve experimentally. Nevertheless, they give a good insight into eventual conversion when these backward reactions could be avoided (e.g., by quenching, i.e., fast cooling after reaction). Fig. 3A allows us to obtain some insight into what conditions would allow for the highest steady-state conversions, at atmospheric pressure. Two trends can be observed. Firstly, at a high [O]/[O_2] ratio, i.e., above 1 (corresponding to an O_2 dissociation degree above 50%), the conversion is higher, and secondly, a low CO_2 fraction in the mixture, corresponding to a high [O]/[CO_2] ratio, also allows for higher conversion. More specifically, a "band" of optimum conversion can be found in Fig. 3A, depending on the combination of [O]/[O_2] ratio vs CO_2 fraction in the mixture. Interesting to notice this zone seems to give as well the best energy efficiencies (see appendix; Fig. A2). A lower [O]/[O_2] ratio can allow for good conversion in the case of lower CO_2 fractions in the mixture. The maximum conversion is reached at 50% CO_2 fraction in the mixture, and high O_2 dissociation, similar to the values of Fig. 1A. In general, the concept allows for some flexibility when it comes to ratios of [O]/[O_2] vs CO_2 fraction in the mixture, and these are tightly related to the temperature in the gas mixture. As seen in Fig. 3A, the higher conversion band closely follows the bright red band of Fig. 3C, corresponding to 2000 K. When performing simulations at a constant temperature of 2000 K, we achieve a broader range in which high conversion can be achieved, allowing even high conversion at lower [O]/[O_2] ratios, as seen in Figs. 3D and 3E. Yet, on a longer timescale, a constant high temperature is detrimental, because it also promotes backward reactions (recombination of CO and O/O_2 back into CO_2). However, temperature control offers here a solution as well: by cooling the gas mixture, we can avoid the backward reactions and achieve a higher steady-state conversion (see Fig. 3E). Temperature control even allows for achieving high conversion at lower pressures without extra cooling, as seen in Fig. 3F. Therefore, this highlights again that temperature, along with O/O_2/CO_2 fractions in the mixture, is an important player in achieving optimal conversion in the system.

3.3. Sensitivity of the results

To get a better insight into how the vibrational levels affect the results, we removed all vibrationally excited species from the chemistry set, As expected, since we study a regular (heated) gas, and not a plasma (that could be in non-thermal equilibrium), the removal of the vibrational levels did not result in any significant changes. A similar result can be found for the addition of O_3 as extra species. In theory, O_3 could be seen as an atomic oxygen source. Moreover, O_3 is a secondary product formed through $O_2 + O$. Additionally, O will react faster with O, than O_3 to form O_2 (the reaction rates are one order higher). This explains why it has limited influence on our results.

When we compare the results of the different chemistry sets, we do obtain clear differences in absolute values. We ran three different sets, as adopted from Butylkin [22], GRI-MECH [23] and Kozàk et al. [24] Moreover, we identified three reactions as a common factor in those three sets, hence we varied those in our set too by a factor 10 (i.e., 10 times higher and 10 times lower). We observe that the general trend stays the same, but the absolute values do vary. Worth noting is that in our set, to keep the study simple, we always changed the complete reaction thus the forward and reverse rates.

In general, we can conclude that the absolute conversion results do change when the rate coefficients are changed, however, the trend of a higher maximum conversion at a certain O fraction seems to stay the same. This is in line with a bigger uncertainty study performed by Berthelot et al. [25]. Table 2.

4. Applicability of this concept

Our results are in line with other observations in plasma research. Our model indeed reveals that the recombination of CO with O_2 plays a big role in CO_2 reforming, which has also been observed in literature, i.e., the addition of O_2 to a CO_2 plasma had a counterproductive effect on the conversion. [26] Obviously, the removal shows a positive effect. [27,28] This was indeed demonstrated by Mori and Tun, by combining their DBD reactor with SOEC, [27] and recently by our group (Vertongen et al.), for plasma reactors in series. [28] This is indeed another way in which the plasma chemistry community could proceed to enhance CO_2 conversion. On the other hand, our approach is different, and focuses on adding (preferably) O atoms to unreacted CO_2 gas (hence when there is no CO present yet, so that recombination of CO with O/O_2, i.e., the opposite reaction, cannot take place), as a novel way for CO_2 conversion, through reaction (R2). Berthelot et al. [17] and Vargas et al. [29], indeed showed by modelling the importance of reaction (R2), while Van der Steeg et al. [18] proved experimentally the benefits of reaction (R2), being an important contributor to CO_2 conversion in plasma, in line with our results.

To put our theoretical results about mixing O atoms (or an O/O_2 mixture) with CO_2 gas into practice, multiple approaches can be chosen. Namely, one can decide on a hands-off or a more controlled system. A hands-off system, here represented by Fig. 1 and Fig. 3A-C, would allow for conversion without extra control of temperature and pressure. This allows for easier design possibilities, but it also limits the conditions that can be used. Depending on the starting temperature, the CO_2/O mixture would have to achieve a temperature between 1500 and 2000 K to allow for conversion to happen, thus CO_2/O ratios and pressure will have to be chosen accordingly.

When using a controlled system, temperature control is the most interesting approach. This can be done, on one hand, with a heating

Table 2
Results of our uncertainty study for the calculated CO_2 conversion with different chemistry sets (details in text). Even though the absolute values of the CO_2 conversion vary, we still observe the same trend for all chemistry sets and all cases investigated, so the general message of our paper is qualitatively valid, independent of which set was used.

Set		Maximum conversion (%)		
		10% O/ 90% CO_2	50% O/ 50% CO_2	90% O/ 10% CO_2
Full Set		< 1%	44%	98%
No Vibrational Levels		< 1%	43%	98%
With O_3		< 1%	43%	98%
Butylkin		13%	58%	96%
GRI-MECH		1%	22%	96%
Kozak		< 1%	43%	98%
$CO_2 + O \rightleftharpoons CO + O_2$	x 0.1	< 1%	31%	92%
	x 10	< 1%	55%	99%
$O_2 + M \rightleftharpoons O + O + M$	x 0.1	< 1%	43%	98%
	x 10	< 1%	42%	98%
$CO_2 + M \rightleftharpoons CO + O + M$	x 0.1	< 1%	52%	99%
	x 10	< 1%	33%	95%

system, in case of temperatures that are too low, or on the other hand, by lowering the temperature after the initial reaction, to quench the backward reaction, when temperatures are too high or remain high for too long. This was illustrated in Fig. 3D-F for example. Fig. 3D shows the maximum conversion at a system with controlled heating at 2000 K. However, if this high temperature stays for too long (1 s in our simulations), this will kill the conversion, reaching final values of 0–8%. Therefore, quenching back to 300 K can allow for "freezing" the conversion at higher values, up to 60%, as seen in Fig. 3E. The benefits of quenching have already been discussed by Vermeiren et al. [30] Another approach is using low pressure and high temperatures, which shows a nice build-up of conversion over time, up to 90%, as illustrated in Fig. 3 F. Low pressures, however, did not allow for high conversion in our "hands-off" models, because the temperatures did not reach the 1500–2000 K limit. To summarise, we believe the temperature is the most important factor. Therefore, the choice of correct conditions in a hands-off system, or using a temperature-controlled system would be recommended.

Finally, an equally important choice that should be made is the source of O-atoms. Depending on the technique, the (atomic) oxygen gas could be created at different temperatures, pressures and dissociation degrees. Methods for O_2 dissociation are (but not limited to) plasma technology, catalysts and photodissociation. Firstly, dissociation by plasma offers a lot of possibilities, ranging from the use of different types of plasma reactors to the use of different O_2 admixtures. Gavrilov and al. [31] obtained a dissociation degree of ~40% in a low-pressure arc plasma (less than 1 Pa) in an Ar/O_2 mixture. Kutasi et al. [32] obtained dissociation degrees as high as 60% in a surface-wave microwave discharge, also upon Ar addition. Dedrick and al. [33] used N_2/O_2 mixtures in radio-frequency driven pulsed atmospheric pressure plasmas to create atomic oxygen. The addition of SF_6 to O_2 also showed interesting results: at 2 mTorr total pressure, an [O]/[O_2] ratio of 0.3 was obtained for 10% SF_6 addition by Booth et al. [34] In pure O_2, Booth et al. [35,36] also observed up to 20–30% of O atoms in a 20–40 mA DC discharge at 1 Torr. Secondly, O_2 dissociation could take place as well with the help of a catalyst. For this purpose, a range of different catalysts could be used, such as Au [37–39], RuO_2 [40], TiO_2 [41], Ag [42], Pt [43], SnO_2 [44]. Finally, when looking at nature and the atmosphere, photodissociation of O_2 by ultraviolet radiation takes place, which can be mimicked in the lab with radiation in the region from 200 to 240 nm, the so-called Herzberg continuum. [45–47].

5. Conclusion

We propose here a new approach to CO_2 conversion, based on mixing CO_2 gas with O atoms. The first step would include the creation of O atoms, independently from CO_2. The next step allows for the addition of O atoms to a CO_2 gas or vice/versa. Based on chemical kinetics simulations, we show that O addition to CO_2 gas at room temperature indeed leads to significant CO_2 conversion, e.g., around 40% for 50% O fraction, without applying external power or heating. This is attributed to a beneficial increase in temperature, self-consistently calculated by our model, resulting from O atom recombination, which is an exothermic reaction. This temperature increase provides enough energy for the endothermic reaction of CO_2 with O atoms, yielding $CO + O_2$, to proceed. This reaction is only slightly endothermic, and temperatures of 2000 K are already sufficient for this reaction to proceed in an efficient way, while thermal CO_2 conversion requires more energy (i.e., higher temperatures, of 3000 K and above). Hence, when staying under the thermal conversion limit (i.e., below 3000 K), the conversion is driven by O atoms and turns out to be very efficient. We explored different $O/O_2/CO_2$ mixing ratios to obtain insight into the possible conversions. We found that mixtures with a 50% fraction of CO_2 allow for the best conversion. In addition, the conversion also has a strong temperature dependence. Staying within the desirable range of maximum temperatures of 1500–2500 K allows for flexibility within the $O/O_2/CO_2$ mixing ratios, and even gas pressures.

This paper is only based on chemical kinetics modelling, but we hope the insights revealed by this modelling can serve as a proof of concept and as the first incentive to explore this concept further in practice.

CRediT authorship contribution statement

C. Verheyen: Conceptualization, Formal analysis, Investigation, Methodology, Visualization, Writing – original draft, Writing – review & editing. **K. van 't Veer:** Methodology, Investigation, Writing – review & editing. **R. Snyders:** Supervision, Writing – review & editing. **A. Bogaerts:** Funding acquisition, Supervision, Writing – review & editing.

Declaration of Competing Interest

The authors declare that they have no known competing financial interests or personal relationships that could have appeared to influence the work reported in this paper.

Data Availability

Data will be made available on request.

Acknowledgements

This research was supported by FWO – PhD fellowship-aspirant, Grant 1184820N. We also want to thank Björn Loenders and Joachim Slaets.

Appendix A. Supporting information

Supplementary data associated with this article can be found in the online version at doi:10.1016/j.jcou.2022.102347.

References

[1] National Oceanic and Atmospheric Administration. Trends in Atmospheric Carbon Dioxide. https://gml.noaa.gov/ccgg/trends/ (accessed 2022-05–12).
[2] Rebecca Lindsey; National Oceanic and Atmospheric Administration. Climate Change: Atmospheric Carbon Dioxide. https://www.climate.gov/news-features/understanding-climate/climate-change-atmospheric-carbon-dioxide (accessed 2022-05–12).
[3] Masson-Delmotte, V.; Zhai, P.; Pörtner, H.-O.; Roberts, D.; Skea, J.; Shukla, P.R.; Pirani, A.; Moufouma-Okia, W.; Péan, C.; Pidcock, R.; Connors, S.; Matthews, J.B. R.; Chen, Y.; Zhou, X.; Gomis, M.I.; Lonnoy, E.; Maycock, T.; Tignor, M.; Waterfield, T. *Global Warming of 1.5°C An IPCC Special Report on the Impacts of Global Warming of 1.5°C above Pre-Industrial Levels and Related Global Greenhouse Gas Emission Pathways, in the Context of Strengthening the Global Response to the Threat of Climate Change, Sustainable Development, and Efforts to Eradicate Poverty Edited by Science Officer Science Assistant Graphics Officer Working Group I Technical Support Unit;* 2019. www.environmentalgraphiti.org.
[4] United Nations. The 17 Goals. https://sdgs.un.org/goals (accessed 2022-05–12).
[5] European Union. Eurostat. Sustainable Development in the European Union: Monitoring Report on Progress towards the SDGs in an EU Context; Publications Office of the European Union, 2021.
[6] D. Archer, V. Brovkin, The millennial atmospheric lifetime of anthropogenic CO_2, Clim. Change (2008) 283–297, https://doi.org/10.1007/s10584-008-9413-1.
[7] R.S. Haszeldine, S. Flude, G. Johnson, V. Scott, Negative emissions technologies and carbon capture and storage to achieve the paris agreement commitments, Philos. Trans. R. Soc. A Math. Phys. Eng. Sci. R. Soc. Publ. (2018), https://doi.org/10.1098/rsta.2016.0447.
[8] T. Wilberforce, A. Baroutaji, B. Soudan, A.H. Al-Alami, A.G. Olabi, Outlook of carbon capture technology and challenges, Sci. Total Environ. 657 (2019) 56–72, https://doi.org/10.1016/j.scitotenv.2018.11.424.
[9] M. Bui, C.S. Adjiman, A. Bardow, E.J. Anthony, A. Boston, S. Brown, P.S. Fennell, S. Fuss, A. Galindo, L.A. Hackett, J.P. Hallett, H.J. Herzog, G. Jackson, J. Kemper, S. Krevor, G.C. Maitland, M. Matuszewski, I.S. Metcalfe, C. Petit, G. Puxty, J. Reimer, D.M. Reiner, E.S. Rubin, S.A. Scott, N. Shah, B. Smit, J.P.M. Trusler, P. Webley, J. Wilcox, N. mac Dowell, Carbon capture and storage (CCS): the way forward, *Energy Environ. Sci.* R. Soc. Chem. May 1 (2018) 1062–1176, https://doi.org/10.1039/c7ee02342a.
[10] Z. Zhang, S.Y. Pan, H. Li, J. Cai, A.G. Olabi, E.J. Anthony, V. Manovic, Recent advances in carbon dioxide utilization, Renew. Sustain. Energy Rev. (2020), https://doi.org/10.1016/j.rser.2020.109799.

[11] P. Tcvetkov, A. Cherepovitsyn, S. Fedoseev, The changing role of CO_2 in the transition to a circular economy: review of carbon sequestration projects, Sustainability (2019), https://doi.org/10.3390/su11205834.

[12] R. Snoeckx, A. Bogaerts, Plasma technology – a novel solution for CO $_2$ conversion? Chem. Soc. Rev. 46 (2017) 5805–5863, https://doi.org/10.1039/C6CS00066E.

[13] A. Fridman. Plasma Chemistry, second ed., Cambridge University Press, Drexel, 2008 https://doi.org/10.1017/CBO9781107415324.004.

[14] A. Bogaerts, G. Centi, Plasma technology for CO_2 conversion: a personal perspective on prospects and gaps, Front. Energy Res. Front. Media (2020), https://doi.org/10.3389/fenrg.2020.00111.

[15] D. Adrianto, Z. Sheng, T. Nozaki, Mechanistic study on nonthermal plasma conversion of CO_2, Int. J. Plasma Environ. Sci. Technol. 14 (1) (2020) 1–9, https://doi.org/10.34343/ijpest.2020.14.e01003.

[16] R.I. Asisov, A.K. Vakar, V.K. Jivotov, M.F. Krotov, O.A. Zinoviev, B. v Potapkin, A. A. Rusanov, V.D. Rusanov, A. Fridman, A. non-equilibrium plasma-chemical process of CO 2 decomposition, Proc. USSR Acad. Sci. Transl. 271 (1) (1982).

[17] A. Berthelot, A. Bogaerts, Modeling of CO $_2$ splitting in a microwave plasma: how to improve the conversion and energy efficiency, J. Phys. Chem. C 121 (15) (2017) 8236–8251, https://doi.org/10.1021/acs.jpcc.6b12840.

[18] A. van de Steeg, P. Viegas, A. Silva, T. Butterworth, A. van Bavel, J. Smits, P. Diomede, M. van de Sanden, G. van Rooij, Redefining the microwave plasma-mediated co2reduction efficiency limit: the role of O-CO2association, ACS Energy Lett. 6 (2021) 2876–2881, https://doi.org/10.1021/acsenergylett.1c01206.

[19] B. deB. Darwent, Bond dissociation energies in simple molecules, Gaithersburg (1970), https://doi.org/10.6028/NBS.NSRDS.31.

[20] Pancheshnyi, S.; Eismann, B.; Hagelaar, G.J.M.; Pitchford, L.C. Computer Code ZDPlasKin. University of Toulouse, LAPLACE, CNRS-UPS-INP: Toulouse 2008. http://www.zdplaskin.laplace.univ-tlse.fr.

[21] V. Vermeiren, A. Bogaerts, Improving the energy efficiency of CO 2 conversion in non-equilibrium plasmas through pulsing vincent vermeiren and annemie bogaerts *, J. Phys. Chem. C (2019) https://doi.org/10.1021/acs.jpcc.9b02362.

[22] Y.P. Butylkin, A.A. Grinenko, A.A. Levitskii, L.S. Polak, N.M. Rytova, D. I. Slovetskii, Mathematical-modeling of the kinetics of the thermal-decomposition of carbon-dioxide in an electric-arc discharge and quenching of the products, High. Energy Chem. 13 (6) (1979) 456–461.

[23] Smith, G.P.; Golden, D.M.; Frenklach, M.; Moriarty, N.W.; Eiteneer, B.; Goldenberg, M.; Bowman, C.T.; Hanson, R.K.; Song, S.; Gardiner, W.C.; Lissianski, V. v.; Qin, Z. GRI-Mech. http://www.me.berkeley.edu/gri_mech/ (accessed 2022-11–10).

[24] T. Kozàk, A. Bogaerts, Splitting of CO_2 by vibrational excitation in non-equilibrium plasmas: a reaction kinetics model, Plasma Sources Sci. Technol. 23 (4) (2014), https://doi.org/10.1088/0963-0252/23/4/045004.

[25] A. Berthelot, A. Bogaerts, Modeling of CO $_2$ plasma: effect of uncertainties in the plasma chemistry, Plasma Sources Sci. Technol. 26 (11) (2017), 115002, https://doi.org/10.1088/1361-6595/aa8ffb.

[26] M. Grofulović, B.L.M. Klarenaar, O. Guaitella, V. Guerra, R. Engeln, A rotational raman study under non-thermal conditions in pulsed CO_2-N2 and CO_2-O2 glow discharges, Plasma Sources Sci. Technol. 28 (4) (2019), https://doi.org/10.1088/1361-6595/ab1240.

[27] S. Mori, L.L. Tun, Synergistic CO_2 conversion by hybridization of dielectric barrier discharge and solid oxide electrolyser cell, Plasma Process. Polym. 14 (6) (2017), https://doi.org/10.1002/ppap.201600153.

[28] R. Vertongen, G. Trenchev, R. van Loenhout, A. Bogaerts, Enhancing CO_2 conversion with plasma reactors in series and O2 removal, J. CO_2 Util. 66 (2022), 102252, https://doi.org/10.1016/j.jcou.2022.102252.

[29] J. Vargas, B. Lopez, M. Lino Da Silva, Heavy particle impact vibrational excitation and dissociation processes in CO_2, J. Phys. Chem. A 125 (2) (2021) 493–512, https://doi.org/10.1021/acs.jpca.0c05677.

[30] V. Vermeiren, A. Bogaerts, Plasma-based CO2Conversion: to quench or not to quench? J. Phys. Chem. C. 124 (34) (2020) 18401–18415, https://doi.org/10.1021/acs.jpcc.0c04257.

[31] N. Gavrilov, A. Kamenetskikh, P. Tretnikov, S. Krivoshapko, Increasing the oxygen dissociation degree in the plasma of a pulse-periodic Ar/O2low-pressure arc, Plasma Sources Sci. Technol. 30 (9) (2021), https://doi.org/10.1088/1361-6595/ac12d8.

[32] K. Kutasi, V. Guerra, S.A. Paulo, Theoretical insight into Ar-O2 surface-wave microwave discharges, J. Phys. D Appl. Phys. 43 (17) (2010), https://doi.org/10.1088/0022-3727/43/17/175201.

[33] J. Dedrick, S. Schröter, K. Niemi, A. Wijaikhum, E. Wagenaars, N. de Oliveira, L. Nahon, J.P. Booth, D. O'Connell, T. Gans, Controlled production of atomic oxygen and nitrogen in a pulsed radio-frequency atmospheric-pressure plasma, J. Phys. D Appl. Phys. 50 (45) (2017), https://doi.org/10.1088/1361-6463/aa8da2.

[34] J.P. Booth, O. Joubert, J. Pelletier, N. Sadeghi, Oxygen atom actinometry reinvestigated: comparison with absolute measurements by resonance absorption at 130 Nm, J. Appl. Phys. (1991) 618–626, https://doi.org/10.1063/1.347395.

[35] J.P. Booth, O. Guaitella, A. Chatterjee, C. Drag, V. Guerra, D. Lopaev, S. Zyryanov, T. Rakhimova, D. Voloshin, Y. Mankelevich, Oxygen (3P) atom recombination on a pyrex surface in an O2 plasma, Plasma Sources Sci. Technol. 28 (5) (2019), https://doi.org/10.1088/1361-6595/ab13e8.

[36] J.-P. Booth, A. Chatterjee, O. Guaitella, D. Lopaev, S.M. Zyryanov, A.V. Volynets, T. v Rakhimova, D. Voloshin, A. Chukalovsky, Y.A. Mankelevich, V. Guerra, Quenching of O 2 (b 1 Σ g +) by O(3 P) atoms. Effect of gas temperature, Plasma Sources Sci. Technol. (2022), https://doi.org/10.1088/1361-6595/ac7749.

[37] X. Deng, B.K. Min, A. Guloy, C.M. Friend, Enhancement of O2 dissociation on Au (111) by adsorbed oxygen: implications for oxidation catalysis, J. Am. Chem. Soc. 127 (25) (2005) 9267–9270, https://doi.org/10.1021/ja050144j.

[38] A. Roldán, S. González, J.M. Ricart, F. Illas, Critical size for O2 dissociation by Au nanoparticles, ChemPhysChem 10 (2) (2009) 348–351, https://doi.org/10.1002/cphc.200800702.

[39] Y. Xu, M. Mavrikakis, Adsorption and dissociation of O2 on gold surfaces: effect of steps and strain, J. Phys. Chem. B 107 (35) (2003) 9298–9307, https://doi.org/10.1021/jp034380x.

[40] H. Wang, W.F. Schneider, D. Schmidt, Intermediates and spectators in O 2 dissociation at the RuO 2(110) surface, J. Phys. Chem. C. 113 (34) (2009) 15266–15273, https://doi.org/10.1021/jp903304f.

[41] Epling, W.S.; Peden, C.H.F.; Henderson, M.A.; Dieboldb, U. *Evidence for Oxygen Adatoms on TiO 2 (110) Resulting from O 2 Dissociation at Vacancy Sites;* 1998; Vol. 412.

[42] M. Lee, E. Kazuma, C. Zhang, M. Trenary, J. Takeya, J. Jung, Y. Kim, Dissociation mechanism of a single O2molecule chemisorbed on Ag(110), J. Phys. Chem. Lett. 12 (40) (2021) 9868–9873, https://doi.org/10.1021/acs.jpclett.1c02456.

[43] P.C. Jennings, H.A. Aleksandrov, K.M. Neyman, R.L. Johnston, O2 dissociation on M@Pt core-shell particles for 3d, 4d, and 5d transition metals, J. Phys. Chem. C. 119 (20) (2015) 11031–11041, https://doi.org/10.1021/jp511598e.

[44] B. Slater, C.R.A. Catlow, D.E. Williams, A.M. Stoneham, Dissociation of O2 on the reduced SnO2 (110) surface, Chem. Commun. (4) (2000) 1235–1236, https://doi.org/10.1039/b002039g.

[45] A.J. Alexander, Z.H. Kim, R.N. Zare, Photodissociation of O2 via the herzberg continuum: measurements of O-atom alignment and orientation, J. Chem. Phys. 118 (23) (2003) 10566–10574, https://doi.org/10.1063/1.1574511.

[46] Z. Farooq, D.A. Chestakov, B. Yan, G.C. Groenenboom, W.J. van der Zande, D. H. Parker, Photodissociation of singlet oxygen in the UV region, Phys. Chem. Chem. Phys. 16 (7) (2014) 3305–3316, https://doi.org/10.1039/c3cp54696a.

[47] K. Tonokura, N. Shafer, Y. Matsumi, M. Kawasaki, Photodissociation of oxygen molecules at 226 Nm in the herzberg I system, J. Chem. Phys. 95 (5) (1991) 3394–3398, https://doi.org/10.1063/1.461779.